

Climb of jogs as a rate-limiting process of screw dislocations motion in olivine dislocation creep

Lin Wang^{1,1} and Tomoo Katsura^{2,2}

¹Carnegie Institution for Science

²University of Bayreuth

November 30, 2022

Abstract

Dislocation recovery experiments were conducted on pre-deformed olivine single crystals at temperatures of 1,450 to 1,760 K, room pressure, and oxygen partial pressures near the Ni-NiO buffer to determine the annihilation rates constants for [001] (010) edge dislocations. The obtained rate constants were comparable with those of previously determined [001] screw dislocations. The activation energies for the motion of both dislocations are identical. This suggests that the motion of screw dislocations in olivine is not controlled by cross-slip but by the same rate-limiting process of the motion of edge dislocations, i.e. climb, at low-stress and high-temperature conditions. The diffusivity derived from dislocation climb indicates that dislocation recovery is controlled by pipe diffusion. The conventional climb controlled model for olivine can be applied to the motions of not only edge but also screw dislocations. The softness of the asthenosphere cannot be explained by the cross-slip controlled olivine dislocation creep.

Hosted file

essoar.10501470.2.docx available at <https://authorea.com/users/533278/articles/608592-climb-of-jogs-as-a-rate-limiting-process-of-screw-dislocations-motion-in-olivine-dislocation-creep>

1 **Climb of jogs as a rate-limiting process of screw dislocation motion in olivine**
2 **dislocation creep**

3 Lin Wang^{a, b} and Tomoo Katsura^{a, c}

4

5 ^a Bayerisches Geoinstitut, University of Bayreuth, 95440 Bayreuth, Germany.

6 ^b Geophysical laboratory, Carnegie institution for Science, Washington D.C., 20015, U.S.A.

7 ^c Center for High Pressure Science and Technology Advanced Research, Beijing, 100094, China

8 * Corresponding author.

9 *E-mail address:* liwang@carnegiescience.edu

10

11 Abstract

12 Dislocation recovery experiments were conducted on predeformed olivine single crystals at
13 temperatures of 1,450 to 1,760 K, room pressure, and oxygen partial pressures near the Ni-NiO
14 buffer to determine the annihilation rate constants for [001](010) edge dislocations. The obtained
15 rate constants were found to be comparable to those of previously determined [001] screw
16 dislocations. The activation energies for the motion of both dislocations are identical. This result
17 suggests that the motion of screw dislocations in olivine is not controlled by cross-slip but by the
18 same rate-limiting process of the motion of edge dislocations, i.e., climb, under low-stress, high-
19 temperature conditions. The diffusivity derived from dislocation climb indicates that dislocation
20 recovery is controlled by Si pipe diffusion, rather than Si lattice diffusion. Our results suggest that
21 the conventional climb-controlled model for olivine can be applied to motions of not only edge but
22 also screw dislocations. Therefore, the previous proposed cross-slip model cannot explain the
23 softness of asthenosphere. The diffusivity derived from dislocation climb indicates that dislocation
24 recovery is controlled by pipe diffusion. The conventional climb-controlled model for olivine can
25 be applied to the motions of not only edge but also screw dislocations. The softness of the
26 asthenosphere cannot be explained by cross-slip controlled olivine dislocation creep.

27

28 **Keywords:** dislocation recovery, dislocation creep, temperature dependence, climb controlled
29 model, asthenosphere

30

31 Introduction

32 Geophysical observations regarding geoid (e.g., Hager, 1991) and postglacial rebound (e.g.,
33 Peltier, 1998) have suggested that a soft asthenosphere underlies a rigid lithosphere. Geodynamic
34 modeling (e.g., Becker, 2017; Craig and McKenzie, 1986) have also suggested the same conclusion.

35 The reason for the presence of soft asthenosphere is under debate. Although the simplest
36 explanation cites a weakening of materials due to high temperatures, the results of deformation
37 experiments conducted on dry peridotite implied that high temperatures are insufficient to explain
38 the softness of the asthenosphere (Hirth and Kohlstedt, 2003). ~~Although a~~ popular explanation
39 refers to the hydrous weakening of olivine (e.g., Mackwell et al., 1985; Hirth and Kohlstedt, 2003).
40 ~~However,~~ this has been refuted by recent Si self-diffusion experiments (Fei et al., 2016; Fei et al.,
41 2013) based on the assumption that dislocation creep is controlled by diffusion. Another possible
42 explanation was proposed by Poirier and Vergobbi (1978). The authors suggested that if the cross-
43 slip of dissociated screw dislocations controls olivine dislocation creep, the estimated upper-mantle
44 viscosity would be one order of magnitude lower than that predicted by the climb-controlled model
45 in a stress range from 10 to 100 bar. This property may explain the softness of the asthenosphere.
46 However, no experimental study has tested this hypothesis.

47 Neither diffusion nor deformation experiments can identify the rate-limiting process of
48 motions of screw dislocations. Diffusion does not involve motions of dislocations. Although it is
49 theoretically possible to determine the rate-limiting process of dislocation motions by examining the
50 stress dependence of creep rates (e.g., Hirth and Kohlstedt, 2003), the stress ranges applied in
51 deformation experiments are too narrow. The conventionally used stress exponent of 3.5 for
52 dislocation creep implies a pipe diffusion-controlled mechanism (Hirth and Kohlstedt, 2003, 2015).
53 However, such experiments have a stress range only from 100 to 224 MPa. On the other hand,
54 Kohlstedt and Goetze (1974) found that the stress exponent increases with increasing stress. Poirier
55 (1985, P.139) found that the stress exponent of olivine single crystal dislocation creep varies from
56 2.6 to 3.7 in different studies.

57 In the present study, we conducted dislocation recovery experiments on [001](010) edge
58 dislocations and compared the results with those of [001](010) screw dislocations given by Wang et
59 al. (2016). During recovery, dislocations move on (glide) and out of the slip plane (climb, cross-
60 slip) successively under the influence of internal stress. Therefore, the activation energy determined
61 by this method represents that of the rate-limiting process of dislocation motions. Although the
62 model developed by Poirier and Vergobbi (1978) ~~was~~ based on [100] screw dislocations, the
63 important point in their model is the dissociation, rather than Burgers vector of dislocations.
64 Because dissociation of [001] screw dislocations have been confirmed in olivine (Vander Sande and
65 Kohlstedt, 1976), [001] screw dislocation can be used to test this hypothesis. In addition, most of
66 [100] dislocations ~~these~~ have an edge character at temperatures of less than 1350 °C (Bai and
67 Kohlstedt, 1992; Wang et al., 2016). ~~On the other hand while,~~ [001] dislocations has similar density
68 of edge and screw components (Wang et al., 2016). ~~the similar density of edge and screw~~
69 ~~dislocations in the [001](010) slip system (Wang et al., 2016)~~ This indicates the equivalent
70 importance of both types of dislocations in this slip system. Therefore, we focus on ~~this the~~ [001]
71 (010) slip system in this study (hereafter called *c*-dislocations).

72

73 **Experimental Procedure**

74 The same Pakistan olivine and sample preparation procedures as those of Wang et al. (2016)
75 were employed in this study. The composition of olivine was reported by Gose et al. (2010). The
76 experimental setup used is similar to that used in Wang et al. (2016). The olivine single crystal was
77 oriented by X-ray diffraction and electron backscattered diffraction (EBSD) and then placed in the

78 cell assembly such that the [001] direction and (010) plane were parallel to the shear direction and
79 plane, respectively.

80 Dislocations with the [001] Burgers vector on the (010) plane were produced by experimental
81 deformation using a Kawai-type multianvil apparatus at the University of Bayreuth. The sample
82 assembly was first pressurized to 3 GPa with a press load of 3.6 MN and then heated to a
83 temperature of 1,600 K and held for 15 min to sinter crushable alumina. After this, the assembly
84 was further compressed to a press load of 3.9 MN for 15 min to deform the sample. After
85 deformation, the sample was quenched by switching off the heating power and then decompressed
86 to room pressure for more than 16 hours. Transmission electronic microscopy (TEM) results
87 presented by Wang et al. (2016) found the [001](010) slip system to be successfully activated and
88 dominant using this procedure. The ratio of screw to edge dislocations was 3:2 as reported by Wang
89 et al. (2016).

90 The deformed olivine crystals were cut into eight cubic pieces and paired into four groups, in
91 which the two pieces in each group shared a common (100) plane. One piece from each pair was
92 used to determine the initial dislocation density while the other was used to determine dislocation
93 density after annealing. The annealing experiments were conducted at ambient pressure and
94 temperatures of 1,460 to 1,760 K for 35 min to 24 hours using a gas mixing furnace. The oxygen
95 partial pressure was controlled at 10^{-6} - 10^{-8} MPa, which is near the Ni-NiO buffer, using a CO-CO₂
96 gas mixture. Table 1 summarizes the conditions of the annealing experiments.

97 Dislocations were observed using the oxidation decoration technique (Kohlstedt et al., 1976,
98 Karato 1987). Corresponding areas away from subgrain boundaries on the common (100) plane in
99 initial and annealed pieces of the same group were observed to determine the change in dislocation

100 density before and after annealing. Although dislocations exist mainly as loops in crystals, the high
101 lattice friction in the [001](010) slip system makes the screw and edge components nearly straight
102 in this slip system (Bai and Kohlstedt 1992, sample deformed in [011]_c orientation, Wang et al.,
103 2016, c-deformed sample). This enable us to distinguish the characters of dislocations by using line
104 geometry of dislocations (Ogawa and Karato, 1989). Since [001](010) edge dislocations elongate in
105 the [100] direction, these dislocations show dots contrasted on the (100) plane in backscattered
106 images after decoration. The number of dots per unit area was counted as the dislocation density.

107 Annihilation rate constants were calculated via second-order dislocation recovery kinetics
108 (Karato and Ogawa, 1982; Kohlstedt et al., 1980; Wang et al., 2016)

$$109 \quad k = \frac{\frac{1}{\rho_f} - \frac{1}{\rho_i}}{t}, \quad (2)$$

110 where ρ_f and ρ_i are the dislocation densities after and before annealing, respectively, and t is the
111 annealing time. Due to the thermally activated process, the dislocation annihilation rate constant is
112 assumed to follow the Arrhenius relationship:

$$113 \quad k = k_0 \exp\left(\frac{-E}{RT}\right) \quad (3)$$

114 where k_0 is a constant, E is the activation energy of dislocation annihilation, T is temperature, and R
115 is the gas constant.

116

117 **Results**

118 Table 1 shows experimental results together with the annealing conditions. Dislocation density
119 in the samples before deformation is less than $0.0004 \mu\text{m}^{-2}$, which is negligible in comparison to the
120 dislocation density after deformation (Table 1). Figure 1 a and b shows back-scattered electron

121 images of decorated dislocations in corresponding areas in the samples from the same pair before
122 and after annealing, respectively. *c*-screw dislocations appear as lines and *c*-edge dislocations
123 appear as dots on the (100) plane due to their geometries. A decrease in dislocation density was
124 observed by comparing the images before and after annealing. The water content in the samples
125 before and after annealing was below the detection limit of infrared spectroscopy. The transmission
126 electron microscope images of the dislocation structures after deformation are given in Fig. 4 in
127 Wang et al. (2016).

128 Figure 1c plots the logarithmic rate constants of *c*-edge dislocation annihilation against the
129 reciprocal temperature. The results from the previous dislocation recovery experiments on *c*-screw
130 dislocations (Wang et al., 2016) and of other studies on dislocation recovery kinetics are also plotted
131 in this figure. The dislocation annihilation rate constants of *c*-edge and *c*-screw dislocations are
132 comparable, but those of the *c*-screw are about half an order of magnitude higher than those of the
133 *c*-edge. The temperature dependences for these two dislocations are identical. Their activation
134 energies are $E_{c\text{-edge}} = 400 \pm 20$ kJ/mol and $E_{c\text{-screw}} = 400 \pm 30$ kJ/mol for the *c*-edge and *c*-screw,
135 respectively.

136

137 Discussion

138 The identical activation energies of annihilation rate constants of the *c*-edge and *c*-screw
139 dislocations indicate that the motions of both dislocations are controlled by the same mechanism.
140 Although many transport properties of olivine exhibit activation energies of 300 to 500 kJ/mol (e.g.,
141 Dohmen et al., 2002, 529 ± 41 kJ/mol for silicon self-diffusion, 338 ± 14 kJ/mol for oxygen self-
142 diffusion), they are distinct from those determined in this study (see also the slope in Fig. 3 and

143 references therein). The high accuracy of activation energies obtained in previous studies and the
144 present one allows us to distinguish the rate-limiting mechanisms of different processes.

145 The motion of edge dislocations is controlled by climb at high temperatures and low stresses
146 (e.g., Hull and Bacon, 2001; Kohlstedt, 2006). However, the motion of a pure screw dislocation
147 does not involve climb because screw segments have no specific slip plane (Hull and Bacon, 2001).
148 Since jogs in screw dislocations have an edge character, we propose that the motion of screw
149 dislocation is controlled by the climb of jogs (Fig. 2). A screw dislocation can form a jog by cross-
150 slips to overcome obstacles that it meets during glide (Fig. 2A and 2B). The slip plane of the jog is
151 defined by its dislocation line (\mathbf{J}) and the Burgers vector (\mathbf{b}), which is indicated by the yellow plane.
152 The parent screw dislocation glides in the y direction, and therefore the jog needs to climb in the y
153 direction to move along with its parental dislocation so that the screw dislocation can go through the
154 obstacle (Fig. 2C). This climb of jogs should serve as the rate-limiting process of screw dislocation
155 motions.

156 It should be noted that although the climb of edge dislocation and jog motion of screw
157 dislocation are essentially the same, the density of climbing parts on edge dislocations and that of
158 jogs on screw dislocations may be different, creating differences in the magnitudes of rate
159 constants. Thus, only the slope in the Arrhenius plot can serve as a fingerprint of the essential
160 mechanism of rate-limiting processes in dislocation recovery experiments.

161 Since climb is controlled by diffusion, the diffusivities derived from annihilation rate constant
162 D^R (based on Karato and Ogawan, 1989) were compared with those of silicon and oxygen diffusion
163 in olivine (Fig. 3). None of these data fit D^R well. Instead, D^R falls between silicon lattice and grain
164 boundary diffusivities. This result indicates that the dislocation climb in olivine may be controlled

165 by pipe diffusion. Vacancies, dislocations and grain boundaries are 0-, 1-, and 2-dimensional
166 defects, respectively, the structure distortion near these defects should increase consequently and
167 accordingly the associated Si diffusivity should increase. In addition, the activation energy of D^R
168 obtained in this study is between those of Si lattice (540 kJ/mol, Dohmen et al., 2002) and grain
169 boundary diffusion (~200 kJ/mol, Fei et al., 2015). This result is also consistent with the hypothesis
170 that pipe diffusion controls dislocation climb (Hirth and Kohlstedt, 2015). Although there are no
171 data for pipe diffusion in olivine, the fact that the diffusion coefficient and activation energy of pipe
172 diffusion fall between those of lattice and grain boundary diffusion is well established for oxides
173 (Frost and Ashby, 1983, Table 12.1). The low activation energy of oxygen lattice diffusion (~340 kJ/
174 mol, Dohmen et al., 2002) rules out the possibility that oxygen diffusion controls dislocation climb.

175

176 **Implications**

177 Our results suggested that the conventional climb model can be used to dislocation motions in
178 olivine regardless of dislocation characters. Although only [001] dislocation is studied in this study,
179 the conclusion can be applied to dislocations with different Burgers vectors in olivine. The cross-
180 slip model requires the recombination of dissociated screw dislocations. If the dissociation distance
181 between two partial dislocations is large, the recombination is difficult. In this case, the cross-slip of
182 screw dislocations can be a rate-limiting process (Poirier, 1976). Previous study (Vander Sande and
183 Kohlstedt, 1976) has revealed that the dissociation distances of [001] and [100] dislocation are
184 similar (~4 nm). Therefore, cross-slip cannot be the rate-limiting process for both [100] and [001]
185 dislocations judging from present study. Although dissociation of [010] dislocations has been

186 reported (Fujino et al., 1993), its low abundance makes its effect on olivine dislocation creep less
187 important.

188 ~~It has been proposed that~~The observation that screw dislocation motion in olivine is controlled
189 by climb of jogs indicates that the softness of the asthenosphere ~~can~~cannot be attributed to the
190 cross-slip controlled dislocation creep of olivine (Poirier and Vergobbi, 1978). Other factors, such
191 as melt and water, could explain the softness of asthenosphere (Hirth and Kohlstedt, 2003).
192 Although this explanation is refuted by Si lattice diffusion (Fei et al., 2013), our results indicate that
193 dislocation climb in olivine is controlled by pipe rather than lattice diffusion under dry conditions.
194 Further study on the water effect on dislocation recovery could reconcile the discrepancy between
195 deformation and diffusion experiments results.

196 ~~However, this hypothesis has never been tested. The present study demonstrates that the~~
197 ~~motion of [001] screw dislocations is controlled by the climb of jogs rather than cross-slip,~~
198 ~~suggesting that the cross-slip model is not applicable for such dislocations in olivine. Although the~~
199 ~~cross-slip model is based on [100] dislocations, study of the [001](010) slip system is more relevant~~
200 ~~to asthenosphere conditions. Dislocation structure analyses indicate that most [100](010)~~
201 ~~dislocations have an edge character (Bai and Kohlstedt, 1992, Wang et al., 2016), indicating that~~
202 ~~olivine dislocation creep cannot be controlled by motions of [100] screw dislocation. On the other~~
203 ~~hand, the similar density (Wang et al., 2016) of edge and screw dislocations in the [001](010) slip~~
204 ~~system indicates that both kinds of dislocations are important. Moreover, deformation experiments~~
205 ~~(e.g., Raterron et al., 2007) suggest that this slip system dominates at high pressures. Therefore, we~~
206 ~~conclude that the cross-slip of screw dislocations cannot control the dislocation creep of olivine and~~

207 ~~accordingly cannot explain the softness of asthenosphere. The climb-controlled model can be used~~
208 ~~in olivine dislocation creep regardless of dislocation characters.~~

209 ~~The viscosity of the asthenosphere is extrapolated from dry olivine creep data using a climb~~
210 ~~model is orders of magnitude higher than the estimated value drawn through geophysical~~
211 ~~observation (Hirth and Kohlstedt 2003). The hydrous weakening of olivine has been proposed to~~
212 ~~explain this discrepancy (e.g., Mackwell et al., 1985; Hirth and Kohlstedt, 2003), but this has been~~
213 ~~refuted by recent Si diffusion experiments (Fei et al., 2016; Fei et al., 2013). However, this study~~
214 ~~indicates that pipe diffusion rather than lattice or grain boundary diffusion may control the~~
215 ~~dislocation motions. This conclusion may explain the discrepant results of deformation and~~
216 ~~diffusion experiments. Further studies on the effect of water on dislocation recovery or pipe~~
217 ~~diffusion in olivine are needed to identify the effect of water on olivine rheology and to better~~
218 ~~explain the softness of the asthenosphere.~~

219

220

221

222

223 **Acknowledgments**

224 We thank H. Fischer and R. Njul of BGI for the sample and for assembly preparation. This
225 research was supported through DFG grants to TK (KA3434-3/1, KA3434-3/2, KA3434-7/1 and
226 KA3434-8/1) and with the annual budget of BGI. All data used in this paper are given in Table 1
227 and plotted in Fig. 1c and have been archived at Earth and Space Science Open Archive
228 doi.org/10.1002/essoar.10501470.1.

229

230 **References**

- 231 Bai, Q., and Kohlstedt, D. L., 1992, High-temperature creep of olivine single crystals, 2. dislocation
232 structures: *Tectonophysics*, v. 206, no. 1–2, p. 1-29.
- 233 Becker, T. W., 2017, Superweak asthenosphere in light of upper mantle seismic anisotropy:
234 *Geochemistry, Geophysics, Geosystems*.
- 235 Craig, C. H., and McKenzie, D., 1986, The existence of a thin low-viscosity layer beneath the
236 lithosphere: *Earth and Planetary Science Letters*, v. 78, no. 4, p. 420-426.
- 237 Dohmen, R., Chakraborty, S., and Becker, H.-W. (2002) Si and O diffusion in olivine and
238 implications for characterizing plastic flow in the mantle. *Geophysical Research Letters*,
239 29(21), 2030.
- 240 Farver, J.R., and Yund, R.A. (2000) Silicon diffusion in forsterite aggregates: Implications for
241 diffusion accommodated creep. *Geophysical Research Letters*, 27(15), 2337-2340.
- 242 Fei, H., Koizumi, S., Sakamoto, N., Hashiguchi, M., Yurimoto, H., Marquardt, K., Miyajima, N.,
243 Yamazaki, D., and Katsura, T., 2016, New constraints on upper mantle creep mechanism
244 inferred from silicon grain-boundary diffusion rates: *Earth and Planetary Science Letters*, v.
245 433, p. 350-359.
- 246 Fei, H., Wiedenbeck, M., Yamazaki, D., and Katsura, T., 2013, Small effect of water on upper-
247 mantle rheology based on silicon self-diffusion coefficients: *Nature*, v. 498, no. 7453, p.
248 213.
- 249 Frost, H.J. and M.F. Ashby, *Deformation mechanism maps: the plasticity and creep of metals and*
250 *ceramics*. 1982: Pergamon press.
- 251 [Fujino, K., H. Nakazaki, H. Momoi, S.-i. Karato, and D. L. Kohlstedt \(1993\), TEM observation of](#)
252 [dissociated dislocations with \$b=\[010\]\$ in naturally deformed olivine, *Physics of the earth and*](#)
253 [*planetary interiors*, 78\(1-2\), 131-137.](#)
- 254 Gose, J., Schmaedicke, E., Markowitz, M., and Beran, A., 2010, OH point defects in olivine from
255 Pakistan: *Mineralogy and Petrology*, v. 99, no. 1-2, p. 105-111.
- 256 Hager, B. H., 1991, Mantle viscosity: A comparison of models from postglacial rebound and from
257 the geoid, plate driving forces, and advected heat flux, *Glacial isostasy, sea-level and mantle*
258 *rheology*, Springer, p. 493-513.
- 259 Hirth, G., and Kohlstedt, D., 2003, Rheology of the Upper Mantle and the Mantle Wedge: A View
260 from the Experimentalists, *Inside the Subduction Factory*, American Geophysical Union, p.
261 83-105.
- 262 Hirth, G., and Kohlstedt, D., 2015, The stress dependence of olivine creep rate: Implications for
263 extrapolation of lab data and interpretation of recrystallized grain size: *Earth and Planetary*
264 *Science Letters*, v. 418, p. 20-26.
- 265 Hull, D., and Bacon, D. J., 2001, *Introduction to dislocations*, Butterworth-Heinemann. P.257
- 266 Karato, S., and Ogawa, M., 1982, High-pressure recovery of olivine: implications for creep
267 mechanisms and creep activation volume: *Physics of the Earth and Planetary Interiors*, v. 28,
268 no. 2, p. 102-117.
- 269 Karato, S., Scanning electron microscope observation of dislocations in olivine. *Physics and*
270 *Chemistry of Minerals*, 1987. 14(3): p. 245-248.
- 271 Kohlstedt, D.L., et al., New Technique for Decorating Dislocations in Olivine. *Science*, 1976.
272 191(4231): p. 1045-1046.

273 Kohlstedt, D., Nichols, H., and Hornack, P., 1980, The effect of pressure on the rate of dislocation
274 recovery in olivine: *Journal of Geophysical Research: Solid Earth* (1978–2012), v. 85, no.
275 B6, p. 3122-3130.
276

277 Kohlstedt, D. L., 2006, The Role of Water in High-Temperature Rock Deformation: Reviews in
278 Mineralogy and Geochemistry, v. 62, no. 1, p. 377-396.

279 Kohlstedt, D. L., and Goetze, C., 1974, Low-stress high-temperature creep in olivine single crystals:
280 *Journal of Geophysical Research*, v. 79, no. 14, p. 2045-2051.

281 Mackwell, S.J., Kohlstedt, D.L., and Paterson, M.S. (1985) The role of water in the deformation of
282 olivine single-crystals. *Journal of Geophysical Research-Solid Earth and Planets*, 90(NB13),
283 1319-1333. Peltier, W., 1998, Postglacial variations in the level of the sea: Implications for
284 climate dynamics and solid-earth geophysics: *Reviews of Geophysics*, v. 36, no. 4, p. 603-
285 689.

286 [Poirier, J. \(1976\), On the symmetrical role of cross-slip of screw dislocations and climb of edge](#)
287 [dislocations as recovery processes controlling high-temperature creep, *Revue de Physique*](#)
288 [*Appliquée*, 11\(6\), 731-738.](#)

289 Poirier, J.-P., 1985, Creep of crystals: high-temperature deformation processes in metals, ceramics
290 and minerals, Cambridge University Press.

291 Poirier, J.-P., and Vergobbi, B., 1978, Splitting of dislocations in olivine, cross-slip-controlled creep
292 and mantle rheology: *Physics of the Earth and Planetary Interiors*, v. 16, no. 4, p. 370-378.

293 Raterron, P., Chen, J., Li, L., Weidner, D., and Cordier, P. (2007) Pressure-induced slip-system
294 transition in forsterite: Single-crystal rheological properties at mantle pressure and
295 temperature. *American Mineralogist*, 92(8-9), 1436-1445.

296 [Vander Sande, J., and D. Kohlstedt \(1976\), Observation of dissociated dislocations in deformed](#)
297 [olivine, *Philosophical Magazine*, 34\(4\), 653-658.](#)

298 Wang, L., Blaha, S., Pintér, Z., Farla, R., Kawazoe, T., Miyajima, N., Michibayashi, K., and
299 Katsura, T., 2016, Temperature dependence of [100](010) and [001](010) dislocation
300 mobility in natural olivine: *Earth and Planetary Science Letters*, v. 441, p. 81-90.

301 Weertman, J., 1955, Theory of Steady-State Creep Based on Dislocation Climb: *Journal of Applied*
302 *Physics*, v. 26, no. 10, p. 1213-1217.
303

304 **Figure and table captions**

305 Figure 1. BEIs showing the dislocation density (a) before and (b) after annealing at 1760 K for 35
306 min. The images were taken on the (100) plane. Screw and edge dislocations are shown as lines and
307 dots, respectively, due to the geometries of their dislocation lines. The yellow scale bar denotes 2
308 μm . (c) Logarithmic dislocation annihilation rate constants of *c*-edge dislocations versus reciprocal
309 temperature. The annihilation rate constants of *c*-screw dislocations from Wang et al. (2016) are
310 plotted together. The activation energies for both dislocations are identical, i.e., 400 kJ/mol.
311 Previous results on dislocation recovery are also plotted for comparison.

312

313

314 Figure 2. A schematic diagram showing the jog-climb controlled motion of a screw dislocation. (a)
315 The screw dislocation (blue line) is elongated in the *x* direction, which is parallel to its Burgers
316 vector *b*, and glides in the *y* direction. The blue dot represents the obstacle that the screw dislocation
317 meets during glide. (b) A jog (red segment) elongated in the *z* direction is produced on the screw
318 dislocation to overcome the obstacle. This jog has an edge nature with the same Burgers vector *b* as
319 that of the parental screw dislocation. The yellow area indicates the glide plane of the jog, which is
320 normal to the *y* direction. (c) The jog has to climb out of its glide plane to move along with its
321 parental screw dislocation.

322

323 Figure 3. Logarithmic diffusivity derived from dislocation annihilation rate constants of *c*-edge and
324 *c*-screw dislocations versus reciprocal temperature. Si and O lattice and grain boundary diffusivities
325 are plotted together.

326

327

328 Table 1. Summary of the experimental conditions and results.

329

330 Table 1. Summary of the experimental conditions and results*.

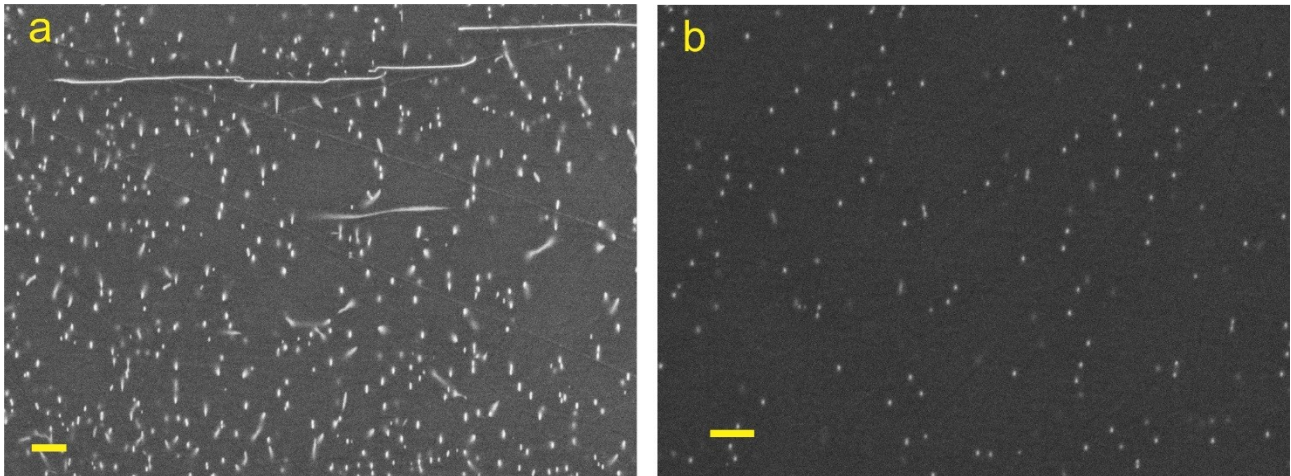
331

[001](010) edge dislocation						
Sample	T (K)	Annealing time (h)	$\log(f_{O_2}, 10^5 \text{ Pa})$	ρ_i (μm^{-2})	ρ_f (μm^{-2})	$\log(k, \text{m}^2\text{s}^{-1})$
Z1643-1	1763	0.58	-4.9	1.60±0.13	0.29±0.01	-14.87±0.03
				0.97±0.13	0.22±0.01	-14.77±0.03
Z1643-2	1673	2.5	-5.7	1.49±0.04	0.36±0.06	-15.63±0.09
				1.13±0.12	0.31±0.03	-15.58±0.05
Z1643-3	1473	24	-7.7	1.33±0.15	0.73±0.05	-17.14±0.09
				0.35±0.03	0.29±0.01	-17.22±0.27

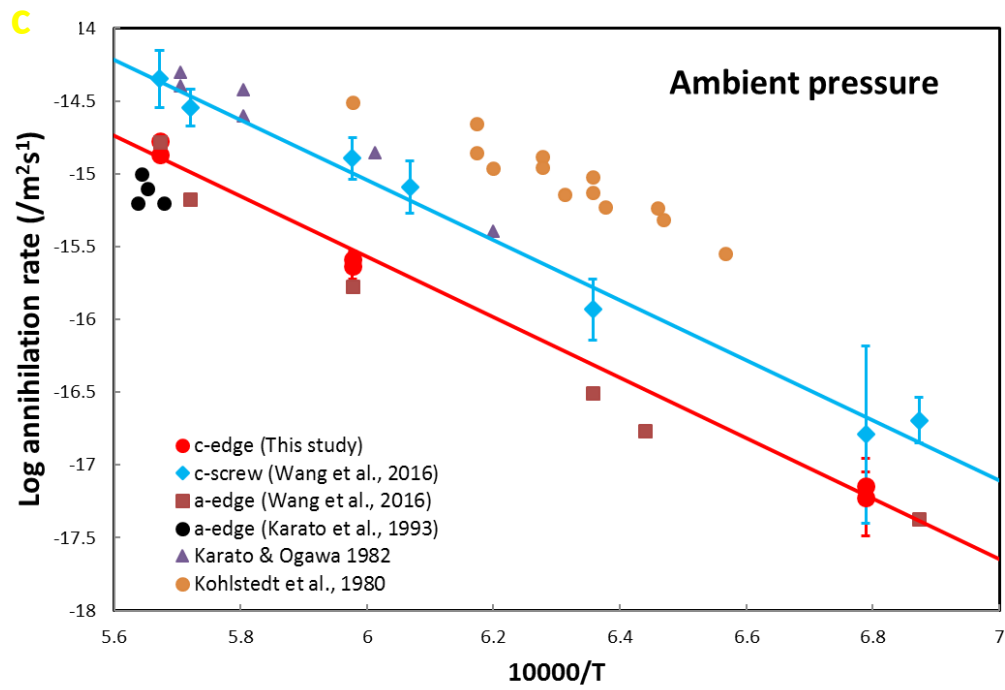
332 * different ρ_i and ρ_f values of each sample correspond to different areas

333

334 Figure 1.



335

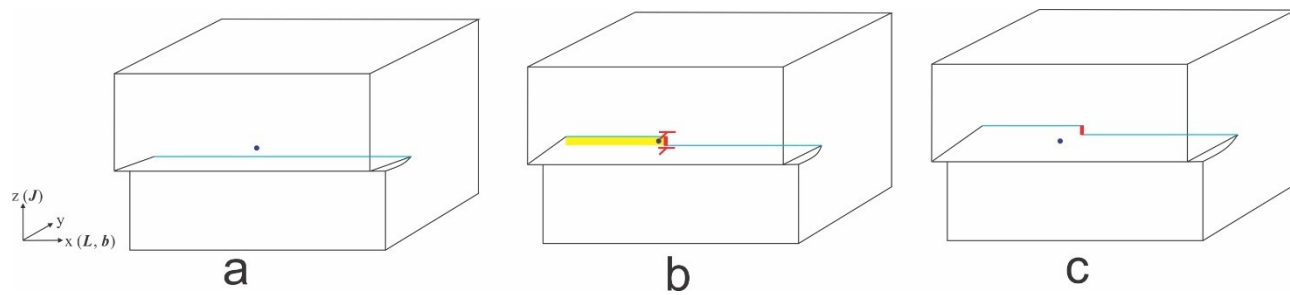


336

337

338

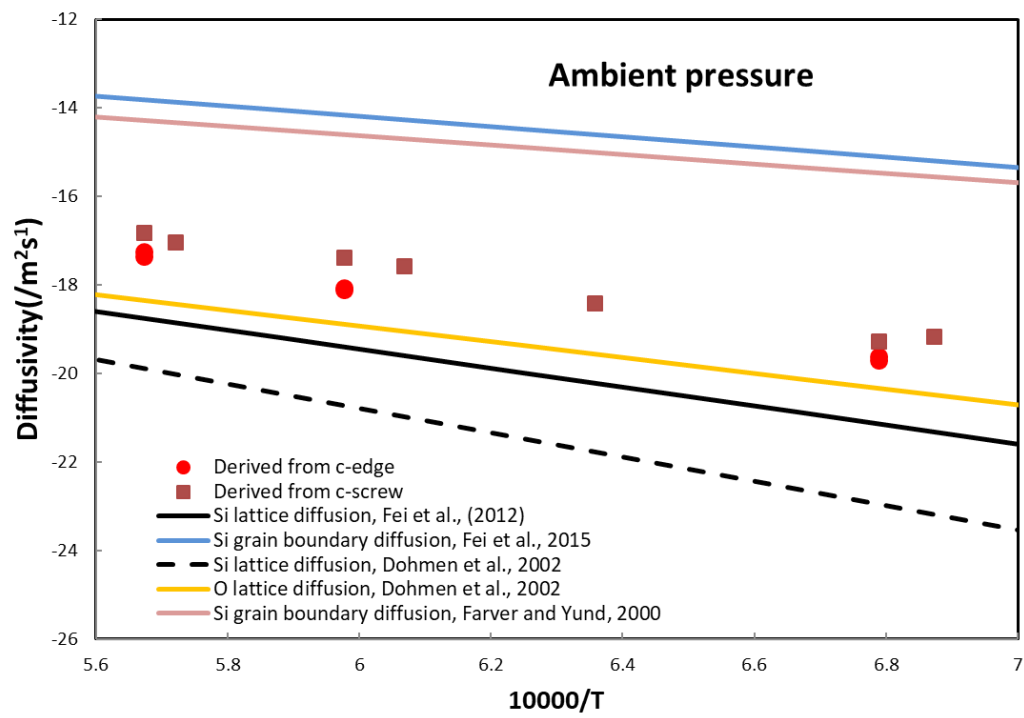
339 Figure 2.



340

341

342 Figure 3.



343